PHYSICAL REVIEW D **96**, 014026 (2017)

# Light cone distribution amplitudes of excited $p$-wave heavy quarkonia at leading twist

M. A. Olpak,[1,*] A. Ozpineci,[2,†] and V. Tanriverdi[2,‡]

[1]*TED University, Basic Sciences Unit, 06420 Ankara, Turkey*
[2]*Middle East Technical University, Department of Physics, 06800 Ankara, Turkey*
(Received 30 August 2016; revised manuscript received 26 May 2017; published 26 July 2017)

Leading twist light cone distribution amplitudes (LCDAs) are key ingredients in calculating various hadronic amplitudes using light cone QCD sum rules. This work concentrates on calculating the leading twist LCDAs of $p$-wave heavy quarkonia. Quark model wave functions for the ground, first, and second excited states of $p$-wave charmonia and bottomonia have been calculated and are used for calculating the relevant LCDAs and leptonic decay constants.

DOI: 10.1103/PhysRevD.96.014026

## I. INTRODUCTION

Understanding hadron structure and spectrum has been one of the major issues in high energy physics for over half a century. Various models have been studied for this purpose up to now, either treating hadrons as fundamental (structureless) particles or composite systems. Today, it is mostly believed that quantum chromodynamics (QCD) is the correct model of the fundamental constituents of hadrons [1,2]. However, it appears to be dramatically difficult to explain hadron structure and spectrum relying solely on QCD, and phenomenological models (such as nonrelativistic or relativized quark models) are still relevant for studies in hadronic physics (e.g., see [3]), although the connection between such models and QCD has not been rigorously established up to now.

The main difficulty in understanding hadron structure is in revealing the source of the confinement phenomenon on theoretical grounds. However, the phenomenon is continuously being demonstrated experimentally (no free quarks or glouns have been detected up to now) and has to be taken into account for understanding properties of hadrons. This issue motivates the use of potential models, which also involve a "confinement potential" [4]. In the seminal paper [4], a "relativized" quark model motivated by QCD is constructed, and the spectrum and various transitions of mesons are calculated.

Due to its nonperturbative nature, nonperturbative methods are necessary to study the hadronic spectrum. One of these methods for analyzing the spectrum and interactions of hadrons is provided by QCD sum rules [5] or its improved light cone QCD sum rules [2,3,6]. However, this method provides reliable information concerning only states that are not radially excited, while there are many known radially excited states in the hadron spectrum. There had been some efforts to study the radially excited states in the literature (see, e.g., [7,8]). Other than potential models, the most promising method for studying excited states (as well as all other properties of the hadron spectrum) is lattice QCD, which also has an extensive literature [3].

All methods concentrate on calculating physically observable quantities related to hadrons and hadron interactions, though they may be regarding part of those as inputs (e.g., a number of hadron masses) for the calculations. Hadron interactions constitute part of the observables involving hadrons. In light cone QCD sum rules, these interactions are expressed in terms of light cone distribution amplitudes (LCDAs) [2,9–23]. Hence, it is of crucial importance to be able to calculate these LCDAs for the hadrons. One proposed way to obtain leading-twist LCDAs is to use the nonrelativistic quark model wave functions obtained through some potential quark models [21,23,24]. One advantage of this approach is that it also allows one to obtain the LCDAs of the radially excited states [21].

As more and more heavier quarkonia are being discovered in experiments, the question of radial excitation attracts attention. Excitations above open flavor thresholds especially present a puzzle for the potential quark model calculations. There are indications that some of these quarkonia, close to or above thresholds, contain both a molecular component, and a quarkonium component [3,25,26]. Although these quarkonium components themselves are not directly observable in nature, to study these mixed quarkonium-molecular systems, it is necessary to know the couplings of the quarkonium component to the molecular component [25,26]. LCDAs obtained through wave functions calculated using potential quark models can be a window to study such systems.

In light cone QCD sum rules, to study the coupling of the hadron $H$ to those which can be created by the currents $j$ and $j'$, a correlation function of the form

*Corresponding author.
maliolpak@gmail.com
†ozpineci@metu.edu.tr
‡tanriverdivedat@googlemail.com

 

$$F(p,q) = i\int d^4x e^{-iq\cdot x}\langle 0|Tj'(x)j^\dagger(0)|H(p)\rangle \quad (1)$$

is analyzed [2,9,10,14–16]. In Eq. (1), the hadron $H(p)$ is on shell. Such correlation functions reduce to expressions involving LCDAs once an expansion around $x^2 = 0$ is performed [2,9,10,14–16]. Such an expansion allows one to perform a partial summation of the operators appearing in a usual $x = 0$ expansion in terms of their twist, which is defined as the difference between the dimension and spin of an operator [2]. Although a sum rules approach can be used for calculating the LCDAs as well (e.g., [19–23]), LCDAs corresponding to excited states cannot be calculated using this method. Relating the LCDAs to nonrelativistic potential models circumvents this difficulty.

The connection between wave functions (calculated by any means, not necessarily using a potential model) and LCDAs has already been studied (e.g., see [24]). In [24], ground state $p$-wave quarkonium wave functions obtained using a variational wave function have been used to obtain the LCDAs. In [21], excited $s$-wave charmonia are studied. However, LCDAs corresponding to the excited $p$-wave quarkonium states are still to be discussed. In this work, relations between the quark model wave functions and leading-twist LCDAs obtained in [24] are used. The quark model wave functions are obtained by explicitly solving the model presented in [4].

This work is organized as follows. In Sec. II, definitions of light cone coordinates and main results obtained in [24] are summarized. In this section, the quark model of [4] is also presented shortly. Section III is devoted to the numerical analysis of our results and describing model functions for the LCDAs. Finally, we conclude our work in Sec. IV.

## II. LEADING TWIST LIGHT CONE DISTRIBUTION AMPLITUDES FOR $p$-WAVE QUARKONIA

The components of some four-vector $k$ in light cone coordinates are defined as [9–13,24]

$$k^\pm \equiv k^0 \pm k^3, \qquad \vec{k}_\perp = (k^1, k^2). \quad (2)$$

For a system of particles having total momentum $P$, one can define the light cone momentum fractions $u_i$ as

$$u_i \equiv k_i^+/P^+ \quad (3)$$

where $k_i$ are the momenta of the constituents. The LCDAs, as functions of these light cone momentum fractions, are obtained by integrating over the transverse momenta. Defined in such a way, they are frame-independent quantities [9–13,24].

For the wave functions, one considers the quark-gluon Fock states carrying the quantum numbers of the hadron, and calculates the LCWFs of each state contributing to the hadron state as follows [9–13,24]:

$$\begin{aligned}&|M(P;{}^{2S+1}L_{J_z},J_z)\rangle\\ &\quad=\sum_{\text{Fock states}}\int\left[\prod_i\frac{dk_i^+d^2k_{\perp,i}}{2(2\pi)^3}\right]2(2\pi)^3\delta^{(3)}\left(\tilde{P}-\sum_i\tilde{k}_i\right)\\ &\qquad\times\sum_{\lambda_i}\Psi_{LS}^{JJ_z}(\tilde{k}_i,\lambda_i)|\text{relevant Fock state}\rangle, \quad (4)\end{aligned}$$

where $\tilde{k} = (k^+, \vec{k}_\perp)$ and $\Psi_{LS}^{JJ_z}(\tilde{k}_i)$ are the light cone wave functions corresponding to the given hadron quantum numbers and relevant Fock states. When one wishes to calculate hadronic couplings, one encounters matrix elements of the form [2,17–23] $\langle q'\bar{q}(p,\epsilon)|\bar{q}'(x)\Gamma q(y)|0\rangle$. For lightlike separations $x-y$, this matrix element can be written as

$$\begin{aligned}&\langle q'\bar{q}(p,\epsilon)|\bar{q}'(x)\Gamma q(y)|0\rangle\\ &\quad=-f_{q'\bar{q}}\int_0^1 du\exp(iup\cdot x+i\bar{u}p\cdot y)\Phi(u,\mu)V[\Gamma], \quad (5)\end{aligned}$$

where $\Phi(u,\mu)$ is the leading-twist distribution amplitude of the $q'\bar{q}$ system, $\mu$ is the scale at which $\Phi(u,\mu)$ is calculated, and $V[\Gamma]$ represents the Lorentz structure related to the Dirac matrix structure $\Gamma$ and possible other factors. Through the hadron states, wave functions enter the calculation, and one can obtain corresponding LCDAs in terms of the relevant wave functions.

In [24], a detailed analysis is presented on how to relate the wave functions to the LCDAs. For completeness, main points in their derivation is presented below. Leading-twist distribution amplitudes of $p$-wave heavy quarkonia are extracted from the following matrix elements:

$$\langle 0|\bar{q}(-z)\gamma^\mu z_\mu q(z)|S(P)\rangle|_{z^2=0} = f_S P\cdot z\int_0^1 du e^{i\xi Pz}\phi_S(u,\mu), \quad (6)$$

$$\langle 0|\bar{q}(-z)\gamma^\mu\gamma_5 z_\mu q(z)|A(P,\epsilon_{\lambda=0})\rangle|_{z^2=0} = if_A M_A\epsilon\cdot z\int_0^1 du e^{i\xi Pz}\phi_{A\parallel}(u,\mu), \quad (7)$$

$$\langle 0|\bar{q}(-z)\gamma^\mu z_\mu q(z)|T(P,\epsilon_{\lambda=0})\rangle|_{z^2=0} = f_T M_T^2\frac{\epsilon^{\mu\nu}z_\mu z_\nu}{P\cdot z}\int_0^1 du e^{i\xi Pz}(1-2u)\phi_{T\parallel}(u,\mu), \quad (8)$$

$$\langle 0|\bar{q}(-z)\sigma^{\mu\nu}\gamma_5\epsilon_{\perp\mu}z_\nu q(z)|A(P,\epsilon_{\lambda=\pm1})\rangle|_{z^2=0} = f_A^\perp \int_0^1 du e^{i\xi P z}\phi_{A\perp}(u,\mu)(\epsilon_\perp\cdot\epsilon_\perp)(P\cdot z), \tag{9}$$

$$\langle 0|\bar{q}(-z)\sigma^{\mu\nu}\epsilon_{\perp\mu\rho}z^\rho z_\nu q(z)|T(P,\epsilon_{\lambda=\pm1})\rangle|_{z^2=0} = i f_T^\perp M_T \int_0^1 du e^{i\xi P z}\phi_{T\perp}(u,\mu)(\epsilon^{\mu\nu}z_\nu\epsilon_{\perp\mu\rho}z^\rho), \tag{10}$$

where $z$ is half the spacetime separation between the quark and the antiquark, $\xi = 1-2u$, $\epsilon^\mu$ and $\epsilon^{\mu\nu}$ are the polarization vector and tensor of the relevant mesons, $P$, $M$, and $f$ are the four-momentum, mass, and decay constant of the relevant mesons, respectively, and [24]

$$\begin{aligned} p_\mu &= P_\mu - z_\mu \frac{M^2}{2P\cdot z}, \\ \epsilon_{\perp\mu} &= \epsilon_\mu - \frac{\epsilon\cdot z}{p\cdot z}\left(p_\mu - z_\mu\frac{M^2}{2p\cdot z}\right), \\ \epsilon_{\perp\mu\nu}z^\nu &= \epsilon_{\mu\nu}z^\nu - \frac{\epsilon_{\mu\nu}z^\mu z^\nu}{p\cdot z}\left(p_\mu - z_\mu\frac{M^2}{2p\cdot z}\right). \end{aligned} \tag{11}$$

The abbreviations $S$, $A$, and $T$ correspond to scalar, axial-vector, and tensor, respectively. Using the C-parity, it can be shown that the distribution amplitudes should have definite symmetry properties under reflections through $u = \frac{1}{2}$. The $p$-wave scalar and tensor mesons have positive C-parities, and hence their distribution amplitudes (DAs) are odd under the exchange of $u \leftrightarrow \bar{u}$, where $\bar{u} = 1-u$. The axial vector can be C-odd or C-even. For C-odd axial vectors $\phi_{A\parallel}$ is odd and $\phi_{A\perp}$ is even, and for C-even axial vectors, $\phi_{A\parallel}$ is even and $\phi_{A\perp}$ is odd.

The matrix elements for the axial-vector and tensor mesons given in [17,18,24] are equivalent, and differ only in notation. However, the Lorentz structure in the matrix elements involves distribution amplitudes having different twists, and it is necessary to disentangle these distribution amplitudes. In [24], an expansion around $z = 0$ has been performed, and the leading terms in those expansions are given in Eqs. (2.26)–(2.28), (2.38)–(2.39). In this work, these matrix elements have been presented for the sake of completeness of the discussion, and so only the fact that $z^2 = 0$ has been used without any expansion around $z = 0$, and Eqs. (6)–(10) have been obtained. Owing to the observations $\epsilon_\perp\cdot z = 0$, $\epsilon_\perp\cdot p = 0$, $\epsilon_{\perp\mu\nu}z^\mu z^\nu = 0$ and $p\cdot z = P\cdot z$ when $z^2 = 0$, one obtains the expressions in Eqs. (6)–(10).

Taking only the quark-antiquark component of the quarkonia, leading-twist distribution amplitudes are related to the quark model wave function through [24] as follows:

$$\phi_{^3P_0}(u,\mu) = \frac{\sqrt{2}}{f_{^3P_0}}\int\frac{d^2\kappa_\perp}{2(2\pi)^3}\frac{(1-2u)m_q}{\sqrt{u\bar{u}}}\varphi_{^3P_0}(u,\vec{\kappa}_\perp), \tag{12}$$

$$\phi_{^3P_1\parallel}(u,\mu) = \frac{2\sqrt{3}}{f_{^3P_1\parallel}}\int\frac{d^2\kappa_\perp}{2(2\pi)^3}\frac{\kappa_\perp^2}{\sqrt{u\bar{u}}M_0(m_q,u,\vec{\kappa}_\perp)} \times\varphi_{^3P_1\parallel}(u,\vec{\kappa}_\perp), \tag{13}$$

$$\phi_{^1P_1\parallel}(u,\mu) = \frac{\sqrt{6}}{f_{^1P_1\parallel}}\int\frac{d^2\kappa_\perp}{2(2\pi)^3}\frac{(1-2u)m_q}{\sqrt{u\bar{u}}}\varphi_{^1P_1\parallel}(u,\vec{\kappa}_\perp), \tag{14}$$

$$\phi_{^3P_2\parallel}(u,\mu) = \frac{\sqrt{6}}{f_{^3P_2\parallel}}\int\frac{d^2\kappa_\perp}{2(2\pi)^3}\frac{(1-2u)}{\sqrt{u\bar{u}}} \times\left[M_0(m_q,u,\vec{\kappa}_\perp) - m_q - \frac{\kappa_\perp^2}{M_0(u,\vec{\kappa}_\perp)+2m_q}\right] \times\varphi_{^3P_2\parallel}(u,\vec{\kappa}_\perp), \tag{15}$$

$$\phi_{^3P_1\perp}(u,\mu) = \frac{\sqrt{3}}{f_{^3P_1\perp}}\int\frac{d^2\kappa_\perp}{2(2\pi)^3}\frac{(1-2u)m_q}{\sqrt{u\bar{u}}}\varphi_{^3P_1\perp}(u,\vec{\kappa}_\perp), \tag{16}$$

$$\phi_{^1P_1\perp}(u,\mu) = \frac{\sqrt{6}}{f_{^1P_1\perp}}\int\frac{d^2\kappa_\perp}{2(2\pi)^3}\frac{\kappa_\perp^2}{\sqrt{u\bar{u}}M_0(m_q,u,\vec{\kappa}_\perp)} \times\varphi_{^1P_1\perp}(u,\vec{\kappa}_\perp), \tag{17}$$

$$\phi_{^3P_2\perp}(u,\mu) = \frac{\sqrt{6}}{f_{^3P_2\perp}}\int\frac{d^2\kappa_\perp}{2(2\pi)^3}\frac{(1-2u)}{\sqrt{u\bar{u}}} \times\left[m_q + \frac{2\kappa_\perp^2}{M_0(m_q,u,\vec{\kappa}_\perp)+2m_q}\right]\varphi_{^3P_2\perp}(u,\vec{\kappa}_\perp), \tag{18}$$

where $m_q$ is the mass of the quark, $\mu$ enters as the upper limit of $k_\perp$ integration (see, e.g., [10]), $\varphi_{\mathcal{M}}(m_q,u,\vec{\kappa}_\perp)$ is the wave function of the state $\mathcal{M}$, and

$$M_0^2 = \frac{m_q^2+\kappa_\perp^2}{u} + \frac{m_q^2+\kappa_\perp^2}{\bar{u}}. \tag{19}$$

In Eqs. (12)–(18), spectral notation is used such that the scalar meson $S$ is the $^3P_0$ state, the axial vector mesons are the $^3P_1$ and $^1P_1$ states, and the tensor meson is the $^3P_2$ state. The leptonic decay constants can be obtained through the normalization condition for the distribution amplitudes,

$$\begin{aligned} \int_0^1 du\phi_{\text{even}}(u,\mu) &= 1, \\ \int_0^1 du(1-2u)\phi_{\text{odd}}(u,\mu) &= 1, \end{aligned} \tag{20}$$

where $\phi_{\text{even(odd)}}$ is a distribution amplitude that is even(odd) with respect to $u = \frac{1}{2}$.

The functions $\varphi_{\mathcal{M}}$ used in Eqs. (12)–(18) can be related to the quark model wave functions as follows. Let

$$\varphi_{\mathcal{M}}(u,\kappa_\perp) = \varphi_p(u,\kappa_\perp)\kappa_{L_3}(u,\kappa_\perp) \tag{21}$$

where $\kappa_{L_3=\pm1} = (\kappa_1 \mp i\kappa_2)/\sqrt{2}$ and $\kappa_{L_3=0} = \kappa_3(u,\kappa_\perp)$.

If $K(|\vec{k}|)$ is the radial function calculated in terms of the standard Minkowski coordinates, the function $\varphi_p$ can be related to the function $K(|\vec{k}|)$ as

$$\varphi_p(u,\kappa_\perp) = A \times \sqrt{\frac{\partial\kappa_z}{\partial u}(u,\kappa_\perp)}\frac{K(|\vec{\kappa}|(u,\kappa_\perp))}{|\vec{\kappa}|}, \tag{22}$$

where $|\vec{\kappa}|(u,\kappa_\perp)$ is the relative momentum of the quark and antiquark, and $A$ is the normalization constant that can be obtained using the normalization condition for the functions $\varphi_{\mathcal{M}}$,

$$\int \frac{dud^2\kappa_\perp}{(2\pi)^3}\varphi_{\mathcal{M}}(u,\kappa_\perp)\varphi^*_{\mathcal{M}'}(u,\kappa_\perp) = \delta_{\mathcal{M}\mathcal{M}'}. \tag{23}$$

Note that, for a given radial excitation quantum number, and ignoring the effect of any spin or angular momentum dependent potentials, all the states considered in this work have the same $\varphi_p$. Under this assumption, the following relations between the leptonic decay constants and LCDAs are expected at the leading twist and at scale $\mu = m_q$ (where $m_q$ is the relevant quark mass) [23,24],

$$\begin{aligned} \sqrt{3}f_{{}^3P_0} &= f_{{}^1P_1\parallel} = \sqrt{2}f_{{}^3P_1\perp} \equiv f_{\text{odd}}, \\ \frac{f_{{}^3P_1\parallel}}{\sqrt{2}} &= f_{{}^1P_1\perp} \equiv f_{\text{even}}. \end{aligned} \tag{24}$$

$$\begin{aligned} \phi_{{}^3P_0} &= \phi_{{}^1P_1\parallel} = \phi_{{}^3P_1\perp} \equiv \phi_{\text{odd}}, \\ \phi_{{}^3P_1\parallel} &= \phi_{{}^1P_1\perp} \equiv \phi_{\text{even}}. \end{aligned} \tag{25}$$

Up to this point, relations between quark model wave functions and LCDAs are discussed. As a result, once the quark model wave function for a state is calculated, its leading twist distribution amplitudes can be obtained through Eqs. (12)–(18). In this work, quark model wave functions calculated using the Godfrey-Isgur Hamiltonian have been used. The Hamiltonian presented in [4] can be written as

$$H = H_0 + H_{ij}^{\text{conf.}} + H_{ij}^{\text{hyp.}} + H_{ij}^{\text{so}}, \tag{26}$$

where $H_0$ is the relativistic kinetic energy, $H_{ij}^{\text{conf.}}$ is the confinement potential, $H_{ij}^{\text{hyp.}}$ is the hyperfine potential, and $H_{ij}^{\text{so}}$ is the spin-orbit interaction. By construction, this Hamiltonian is written in the meson rest frame so that its eigenvalues correspond directly to meson masses. Eigenfunctions of the 3-dimensional simple harmonic oscillator are chosen as the basis in which this Hamiltonian is to be diagonalized. In terms of this basis, the eigenstates can be written as

$$\begin{aligned} \Psi^{QM}(\vec{\kappa};n,L,S,J,J_z) = &\sum_{L_z,S_z} \mathrm{C} \times \langle L,L_z;S,S_z|L,S,J,J_z\rangle \times \chi_{S,S_z} \times Y_{L,L_z}(\theta_\kappa,\phi_\kappa) \\ &\times \sum_{m=0}^{N} h_{nm}\sqrt{2\times\frac{2}{\nu^3}\frac{m!}{\Gamma(m+L+\frac{1}{2})[2(L+m)+1]}}(\nu\kappa)^L \exp\left[-\frac{\kappa^2}{2\nu^2}\right] \mathrm{L}_m^{l+1/2}\left(\frac{\kappa^2}{\nu^2}\right), \end{aligned} \tag{27}$$

where $\vec{\kappa}$ is the relative momentum of the quarks, $\mathrm{L}_m^{l+1/2}(\frac{\kappa^2}{\nu^2})$ are Laguerre polynomials, $Y_{L,L_z}(\theta_\kappa,\phi_\kappa)$ are spherical harmonics in momentum space, $n$ is the radial quantum number, $\mathrm{C} = \frac{1}{\sqrt{3}}(R\bar{R} + B\bar{B} + G\bar{G})$ is the color part, and $\chi_{S,S_z}$ is the spin part of the wave function. To make a numerical diagonalization of the Hamiltonian possible, the Hamiltonian matrix is truncated by keeping only the first $N = 16$ states in the corresponding block specified by the conserved quantities of the system. $h_{nm}$ are determined by diagonalizing the $N \times N$ Hamiltonian matrix. The parameter $\nu$ appearing in the above expression parametrizes the frequency of the oscillator. Its value is determined as to minimize the ground state energy in the corresponding Hamiltonian block. Dressed $c$ quark and $b$ quark masses are taken to be $m_c = 1628$ MeV, $m_b = 4977$ MeV in our calculations. Other parameters related to the quark model calculations can be found in [4].

Within the above mentioned framework, the spectrum and the wave functions are obtained. The obtained masses for the first three levels are presented in Table I. In Table II, we present the observed masses (if available) for the corresponding states. Comparing the two tables, it is observed that the model is quite

TABLE I. Quark model masses calculated for the first three levels of charmonia and bottomonia.

| Masses | $c\bar{c}$ | | | $b\bar{b}$ | | |
|---|---|---|---|---|---|---|
| $M(\text{GeV})\backslash n$ | $n=1$ | $n=2$ | $n=3$ | $n=1$ | $n=2$ | $n=3$ |
| $M_{{}^3P_0}(\chi_{q0})$ | 3.37 | 3.88 | 4.30 | 9.81 | 10.2 | 10.7 |
| $M_{{}^3P_1}(\chi_{q1})$ | 3.54 | 3.97 | 4.33 | 9.89 | 10.3 | 10.6 |
| $M_{{}^1P_1}(h_q)$ | 3.53 | 3.96 | 4.37 | 9.88 | 10.3 | 10.6 |
| $M_{{}^3P_2}(\chi_{q2})$ | 3.54 | 3.98 | 4.34 | 9.89 | 10.3 | 10.6 |

TABLE II. Masses of experimentally observed states in Particle Data Group listings [27].

| Masses | $c\bar{c}$ | | | $b\bar{b}$ | | |
|---|---|---|---|---|---|---|
| $M$(MeV)\$n$ | $n=1$ | $n=2$ | $n=3$ | $n=1$ | $n=2$ | $n=3$ |
| $M_{^3P_0}(\chi_{q0})$ | 3414.75 | – | – | 9859.44 | 10232.5 | – |
| $M_{^3P_1}(\chi_{q1})$ | 3510.66 | – | – | 9892.78 | 10255.46 | 10512.1 |
| $M_{^1P_1}(h_q)$ | 3525.38 | – | – | 9899.3 | 10259.8 | – |
| $M_{^3P_2}(\chi_{q2})$ | 3556.20 | 3927.2 | – | 9912.21 | 10268.65 | – |

successful in reproducing the observed masses (when available).

## III. NUMERICAL ANALYSIS AND MODEL LCDAS

Once the wave functions are obtained, the calculation of the LCDAs is straightforward. One issue that needs to be addressed is the scale dependence of the LCDAs and decay constants. One can consult the evolution equations relating the LCDAs and decay constants calculated at a generic scale $\mu$ to the ones calculated at some reference scale $\mu_0$ (see, e.g., [10,23]). One can also proceed to a direct calculation for various scales. This latter approach has been adopted in this work, since wave functions calculated in the quark model have been used and the $k_\perp$ integrals in Eqs. (12)–(18) are convergent for all values of the scale $\mu$. In this work, LCDAs and decay constants at scales $\mu = m_{c,b}$ and $\mu = \infty$ have been calculated.

On practical grounds, it is also desirable to express the LCDAs in terms of a few parameters which can be easily tabulated and used. In [23], the following expressions for the LCDAs have been motivated using sum rules techniques (for $\xi$-odd and $\xi$-even LCDAs respectively):

$$\phi_{\mathrm{odd}}(\xi) = c(\beta)(1-\xi^2)\xi \exp\left(-\frac{\beta}{1-\xi^2}\right),$$
$$\phi_{\mathrm{even}}(\xi) = -\int_{-1}^{\xi} dt \phi_{\mathrm{odd}}(t) = \frac{c(\beta)}{2}(1-\xi^2)^2 E_3\left(\frac{\beta}{1-\xi^2}\right), \tag{28}$$

where $E_3(x) \equiv \int_1^\infty dt \frac{e^{-xt}}{t^3}$, and the parameters $c$ and $\beta$ are to be fitted to the LCDAs. In this work, we generalize this model to the excited states as well. The models for even LCDAs are chosen to be

$$\begin{aligned} n=1:\ \psi(\xi) &= a(1-\xi^2)^2\left(E_3\left(\frac{\beta}{1-\xi^2}\right) + b\exp\left(-\frac{\xi^2}{c}\right)\right), \\ n=2,3:\ \psi(\xi) &= a\left\{\frac{1}{1+\frac{(\xi^2-\xi_0^2)^2}{\sigma^2}} + b\exp\left(-\frac{\xi^2}{c}\right)\right\}\exp\left(-\frac{\beta}{1-\xi^2}\right), \end{aligned} \tag{29}$$

and for odd LCDAs,

$$\begin{aligned} n=1:\ \phi(\xi) &= a\xi(1-\xi^2)\left\{\exp\left(-\frac{\beta}{1-\xi^2}\right) + b\exp\left(-\frac{\xi^2}{c}\right)\right\}, \\ n=2,3:\ \phi(\xi) &= -\frac{d}{d\xi}\left\{a\left[\frac{1}{1+\frac{(\xi^2-\xi_0^2)^2}{\sigma^2}} + b\exp\left(-\frac{\xi^2}{c}\right)\right]\exp\left(-\frac{\beta}{1-\xi^2}\right)\right\}. \end{aligned} \tag{30}$$

For $n = 1$, the model functions we use correspond to the model used in [23] when $b = 0$. In [28], alternative model functions are proposed on physical grounds. Using the arguments of [28], for excited states, it is possible to obtain a model for the DAs where the exponential factor $e^{-\frac{\beta}{1-\xi^2}}$ (for odd LCDAs) or $E_3(\frac{\beta}{1-\xi^2})$ (for even LCDAs) is multiplied by a linear combination of various powers of $\sqrt{1-\xi^2}$. To obtain a reliable fit to our LCDAs, it is required to have many terms in this linear combination. The model that we propose, although is not physically motivated, can reproduce our LCDAs reliably with fewer fit parameters.

The results for the relevant leptonic decay constants are presented in Tables III–V. In the tables, both leptonic decay constants, and the leptonic decay constant multiplied by the coefficient, when not equal to one, in the relations presented in Eq. (24) are presented in order to facilitate their comparison.

It is observed that the relations in Eq. (24) are qualitatively satisfied. The largest deviation is observed in $f_{^3P_0}$, which can be as large as, e.g., 50% for the $n = 3$ bottomonium case. The values given in [23,24] and the results of this work agree in the order of magnitude of the numbers. The fact that there is no precise agreement in the decay constants stems from using different model functions to calculate the decay constants and LCDAs. It is also generally observed that the deviations from relations in Eq. (24) are enhanced when $n$ increases but are suppressed when $\mu = m_{c,b}$ is used. Both are expected from spin-orbit effects as in both cases since the model functions

TABLE III. Decay constants $f_{^1P_1}, f_{^3P_0}, f_{^3P_1\perp}$ for relevant charmonia and bottomonia.

| $n\backslash f$(GeV) | $f_{^3P_0}$ | $f_{^3P_1\perp}$ | $f_{^1P_1}$ | $\sqrt{3}f_{^3P_0}$ | $\sqrt{2}f_{^3P_1\perp}$ | $f_{\text{odd}}$ |
|---|---|---|---|---|---|---|
| charmonia | $\mu=\infty$ | | | | | |
| $n=1$ | 0.109 | 0.0959 | 0.142 | 0.189 | 0.136 | 0.118 |
| $n=2$ | 0.0801 | 0.0881 | 0.129 | 0.139 | 0.125 | 0.105 |
| $n=3$ | 0.0755 | 0.0824 | 0.133 | 0.131 | 0.117 | 0.103 |
| | $\mu=m_c$ | | | | | |
| $n=1$ | 0.0916 | 0.0875 | 0.127 | 0.159 | 0.124 | 0.105 |
| $n=2$ | 0.0588 | 0.0741 | 0.107 | 0.102 | 0.105 | 0.0860 |
| $n=3$ | 0.0459 | 0.0615 | 0.0946 | 0.0795 | 0.0870 | 0.0735 |
| bottomonia | $\mu=\infty$ | | | | | |
| $n=1$ | 0.104 | 0.0802 | 0.119 | 0.180 | 0.113 | 0.100 |
| $n=2$ | 0.103 | 0.0832 | 0.124 | 0.178 | 0.118 | 0.104 |
| $n=3$ | 0.131 | 0.0834 | 0.143 | 0.227 | 0.118 | 0.116 |
| | $\mu=m_b$ | | | | | |
| $n=1$ | 0.0972 | 0.0794 | 0.117 | 0.168 | 0.112 | 0.0981 |
| $n=2$ | 0.0976 | 0.0822 | 0.121 | 0.169 | 0.116 | 0.101 |
| $n=3$ | 0.118 | 0.0820 | 0.136 | 0.204 | 0.116 | 0.0951 |

TABLE IV. Decay constants $f_{^1P_1\perp}, f_{^3P_1}$ for relevant charmonia and bottomonia.

| $n\backslash f$(GeV) | $f_{^3P_1}$ | $f_{^1P_1\perp}$ | $\frac{f_{^3P_1}}{\sqrt{2}}$ | $f_{\text{even}}$ | $f_{^3P_1}$ | $f_{^1P_1\perp}$ | $\frac{f_{^3P_1}}{\sqrt{2}}$ | $f_{\text{even}}$ |
|---|---|---|---|---|---|---|---|---|
| charmonia | $\mu=\infty$ | | | | $\mu=m_c$ | | | |
| $n=1$ | 0.264 | 0.199 | 0.187 | 0.232 | 0.185 | 0.133 | 0.131 | 0.159 |
| $n=2$ | 0.279 | 0.209 | 0.197 | 0.244 | 0.143 | 0.101 | 0.101 | 0.122 |
| $n=3$ | 0.290 | 0.246 | 0.205 | 0.268 | 0.0852 | 0.0595 | 0.0603 | 0.0724 |
| bottomonia | $\mu=\infty$ | | | | $\mu=m_b$ | | | |
| $n=1$ | 0.182 | 0.138 | 0.129 | 0.160 | 0.173 | 0.126 | 0.122 | 0.146 |
| $n=2$ | 0.197 | 0.148 | 0.139 | 0.173 | 0.184 | 0.135 | 0.130 | 0.156 |
| $n=3$ | 0.204 | 0.182 | 0.144 | 0.193 | 0.187 | 0.153 | 0.132 | 0.170 |

TABLE V. Decay constants $f_{^3P_2}, f_{^3P_2\perp}$ for tensor charmonia and bottomonia.

| $n\backslash f$(GeV) | $f_{^3P_2}$ | $f_{^3P_2\perp}$ | $f_{^3P_2}$ | $f_{^3P_2\perp}$ |
|---|---|---|---|---|
| charmonia | $\mu=\infty$ | | $\mu=m_c$ | |
| $n=1$ | 0.198 | 0.141 | 0.177 | 0.128 |
| $n=2$ | 0.229 | 0.142 | 0.189 | 0.118 |
| $n=3$ | 0.245 | 0.140 | 0.182 | 0.101 |
| bottomonia | $\mu=\infty$ | | $\mu=m_b$ | |
| $n=1$ | 0.133 | 0.113 | 0.131 | 0.112 |
| $n=2$ | 0.148 | 0.121 | 0.146 | 0.119 |
| $n=3$ | 0.178 | 0.137 | 0.168 | 0.131 |

TABLE VI. Comparison of the spin averaged leptonic decays constant for the ground state charmonium with the results in the literature.

| | [24] | [23] | this work ($\Lambda=\infty$) | this work ($\Lambda=m_c$) |
|---|---|---|---|---|
| $f_{\text{odd}}$ (GeV) | 0.088 | – | 0.118 | 0.105 |
| $f_{\text{even}}$ (GeV) | 0.109 | 0.192 | 0.232 | 0.159 |
| $f_{T\parallel}$ (GeV) | 0.124 | – | 0.198 | 0.177 |
| $f_{T\perp}$ (GeV) | 0.098 | – | 0.141 | 0.128 |

TABLE VII. Comparison of the spin averaged leptonic decays constant for the ground state bottomonium with the results in the literature.

| | [24] | this work ($\Lambda = \infty$) | this work ($\Lambda = m_b$) |
|---|---|---|---|
| $f_{\mathrm{odd}}$ (GeV) | 0.067 | 0.100 | 0.098 |
| $f_{\mathrm{even}}$ (GeV) | 0.072 | 0.160 | 0.146 |
| $f_{T\parallel}$ (GeV) | 0.075 | 0.133 | 0.131 |
| $f_{T\perp}$ (GeV) | 0.069 | 0.113 | 0.112 |

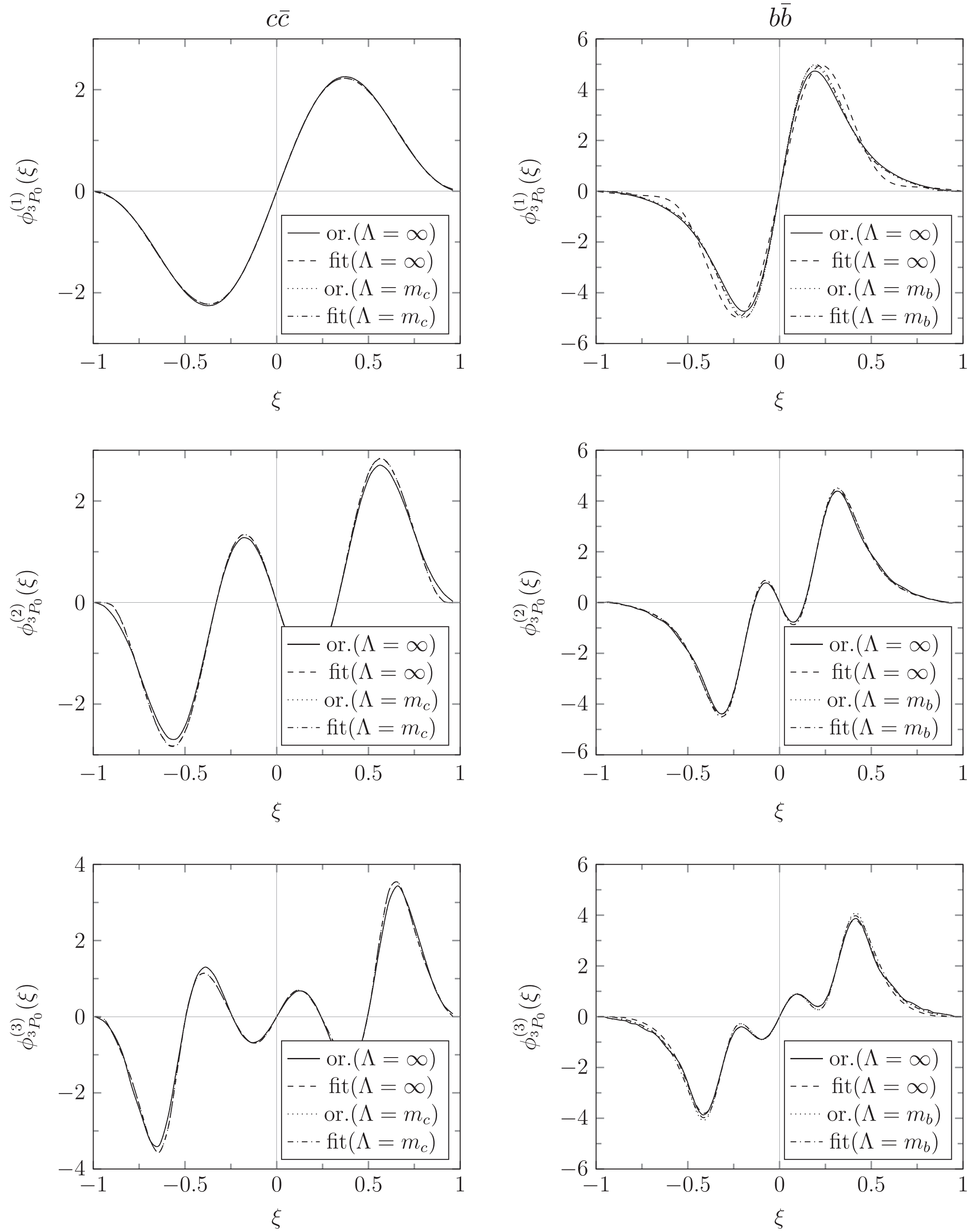


FIG. 1. LCDA plots for $^3P_0$ states. Upper limit of $k_\perp$ integration is indicated in parentheses. "Or." refers to the original function, and "fit" refers to the fitted function. The radial quantum number $n$ is indicated in parentheses as superscript: $\phi^{(n)}(u)$.

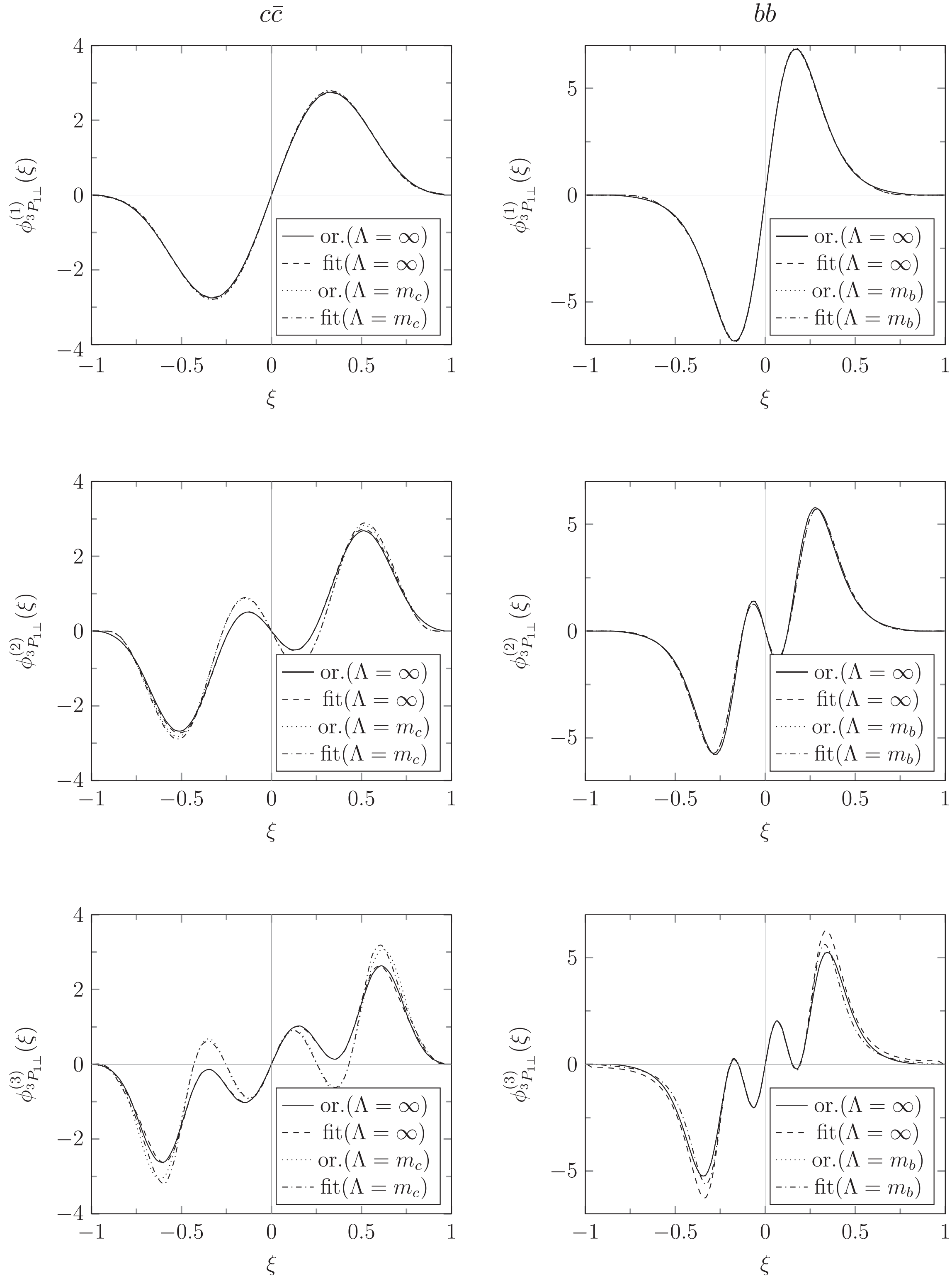


FIG. 2. LCDA plots as in Fig. 1, but for ${}^3P_{1\perp}$ states.

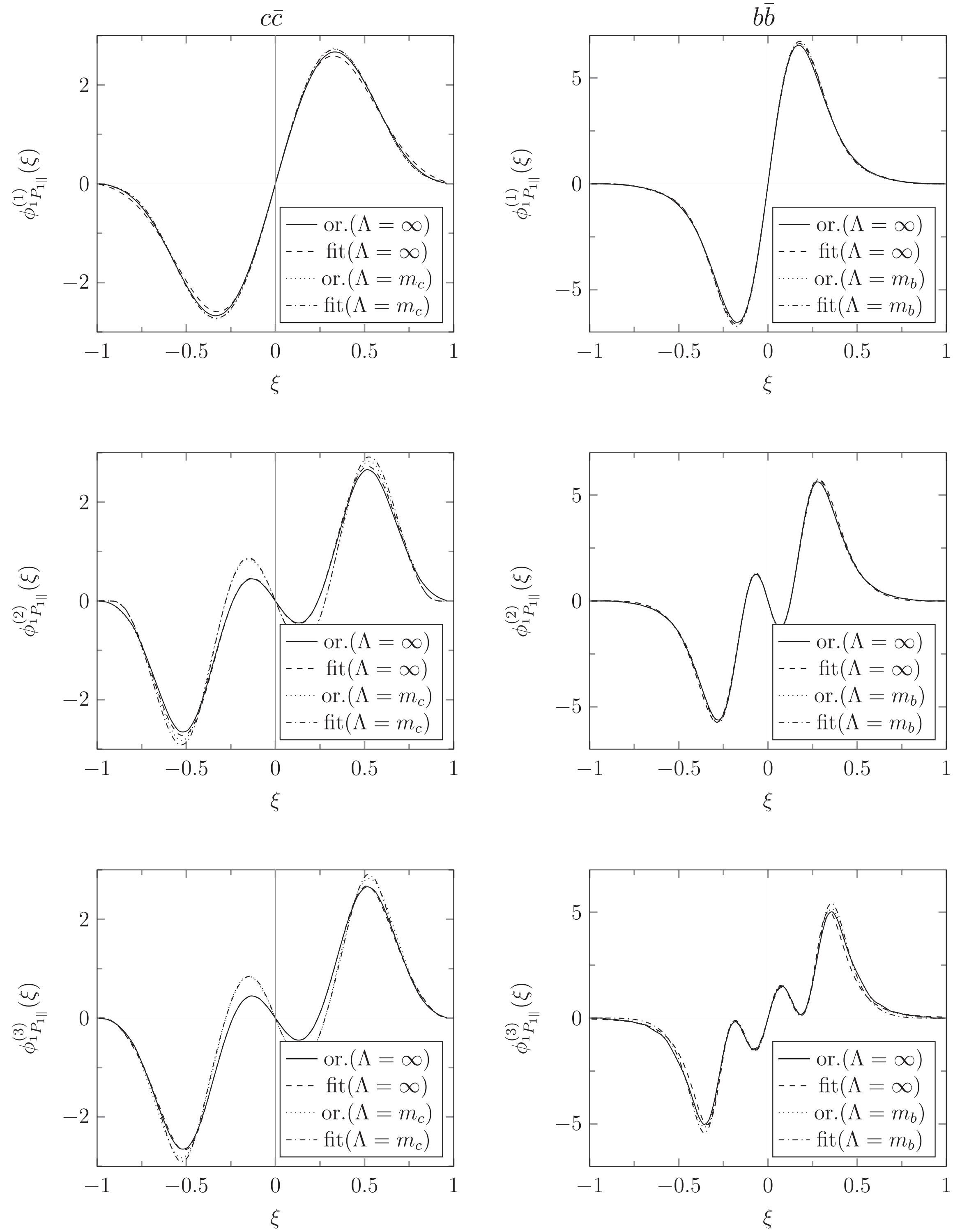


FIG. 3. LCDA plots as in Fig. 1, but for $^1P_{1\parallel}$ states.

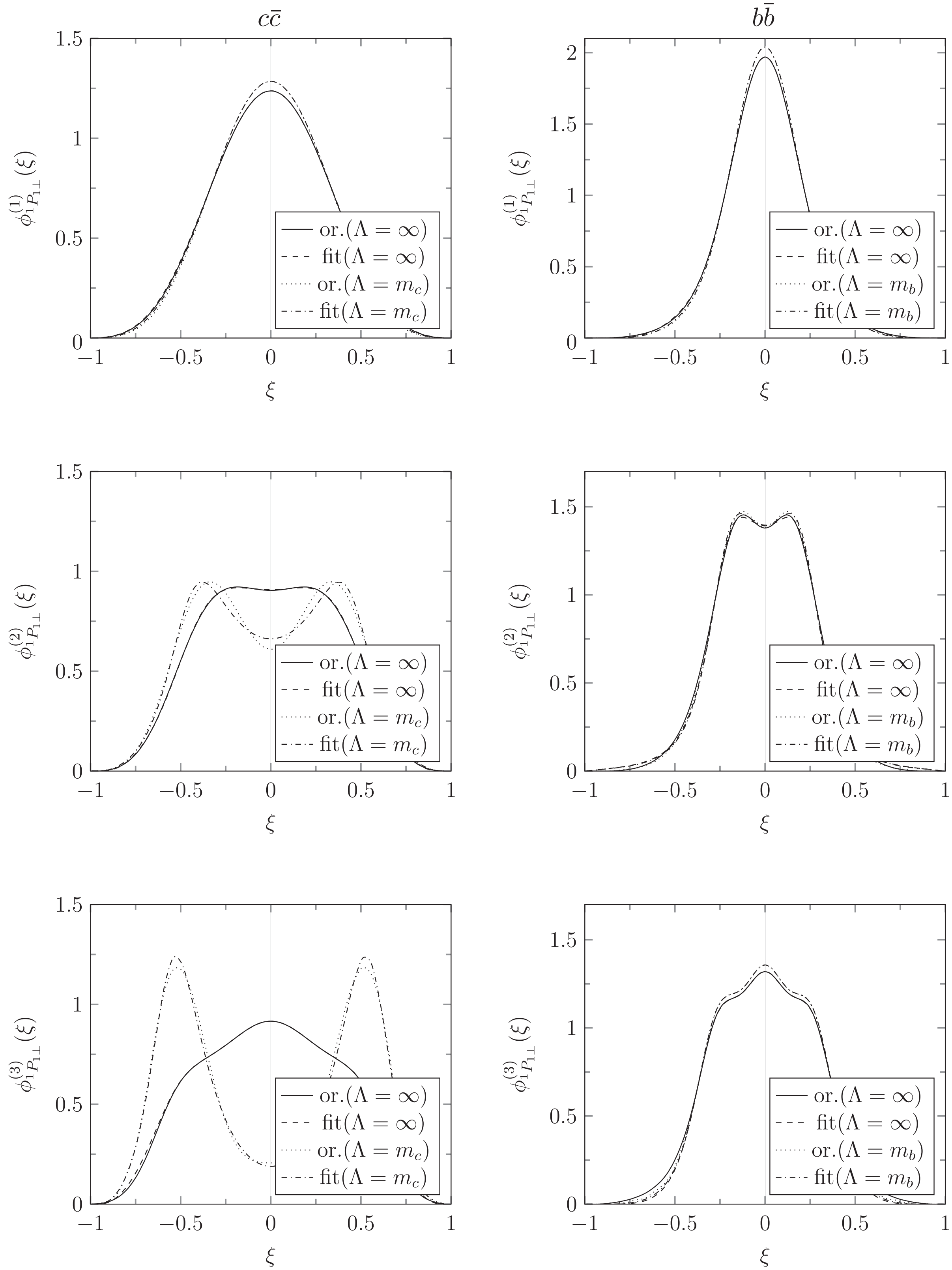


FIG. 4. LCDA plots as in Fig. 1, but for ${}^1P_{1\perp}$ states.

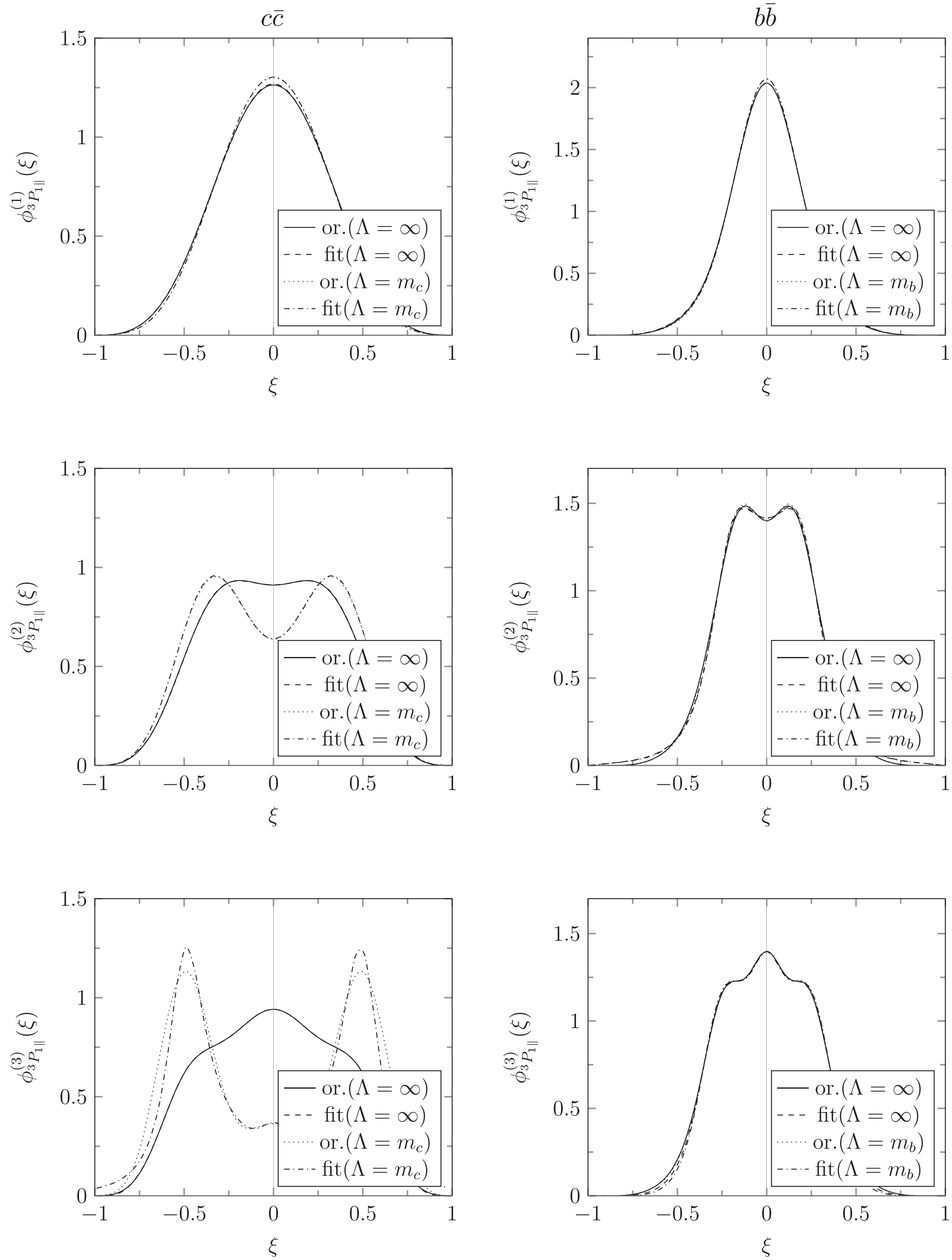


FIG. 5. LCDA plots as in Fig. 1, but for $^3P_{1\parallel}$ states.

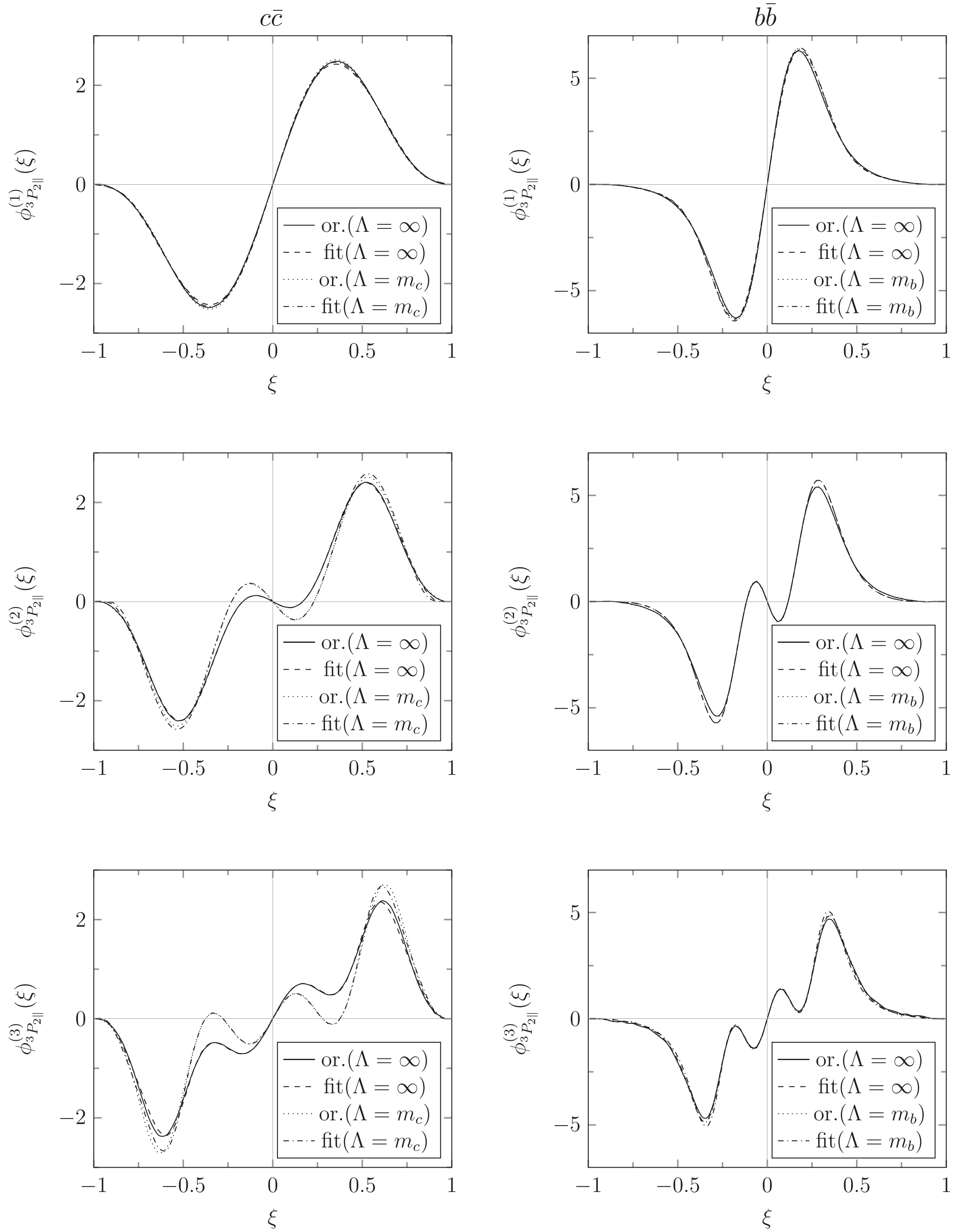


FIG. 6. LCDA plots as in Fig. 1, but for $^3P_{2\parallel}$ states.

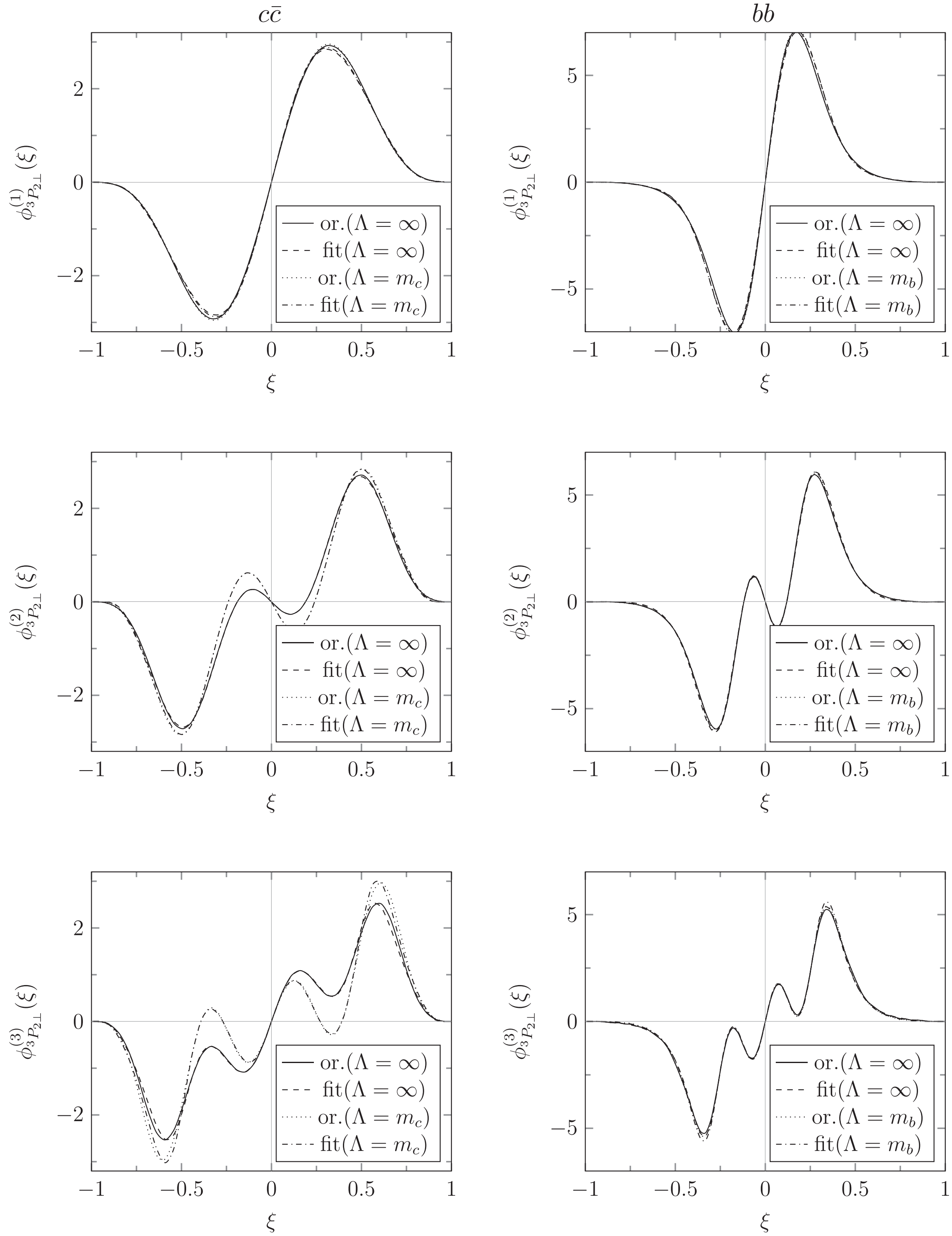


FIG. 7. LCDA plots as in Fig. 1, but for $^3P_{2\perp}$ states.

take spin-orbit effetcs into account. Scale dependence of the leptonic decay constant for the charmonium is apparently more significant compared to the bottomonium sector. Scale dependence of the LCDAs with different radial quantum numbers become more significant as $n$ increases in both sectors, whereas for ground states, scale dependence is not so significant in both sectors. However, the spin weighted average $f_{\mathrm{odd}}$ of charmonium also appears to be slightly affected by the scale.

In [23,24], leptonic decay constants of only the ground states are analyzed ignoring spin-orbit effects. For comparison, we present the spin averaged leptonic decay

TABLE VIII. $^3P_0$ charmonium fit parameters, $\mu = \infty$.

| | $a$ | $\xi_0$ | $\sigma^2$ | $\beta$ | $b$ | $c$ |
|---|---|---|---|---|---|---|
| $n = 1$ | 5.29486 | – | – | 0.867659 | 1.36101 | 0.352628 |
| $n = 2$ | 6.98919 | 0.257499 | 0.182999 | 1.50283 | −0.560786 | 0.149576 |
| $n = 3$ | 1.98475 | 0.51822 | 0.0928117 | 0.847995 | 0.482135 | 0.083937 |

TABLE IX. $^3P_0$ charmonium fit parameters, $\mu = m_c$.

| | $a$ | $\xi_0$ | $\sigma^2$ | $\beta$ | $b$ | $c$ |
|---|---|---|---|---|---|---|
| $n = 1$ | 5.87696 | – | – | 1.00251 | 1.2953 | 0.346534 |
| $n = 2$ | 7.26777 | 0.255466 | 0.185855 | 1.52799 | −0.567534 | 0.152166 |
| $n = 3$ | 2.22227 | 0.538532 | 0.063798 | 0.736003 | 0.262874 | 0.0490782 |

TABLE X. $^3P_0$ bottomonium fit parameters, $\mu = \infty$.

| | $a$ | $\xi_0$ | $\sigma^2$ | $\beta$ | $b$ | $c$ |
|---|---|---|---|---|---|---|
| $n = 1$ | 14.9131 | – | – | 1.29523 | 2.47014 | 0.070175 |
| $n = 2$ | 4.08343 | 0 | 0.018278 | 1.01745 | −0.155892 | 0.0244758 |
| $n = 3$ | 6.5 | 0.288561 | 0.0244281 | 1.70944 | 0.260454 | 0.0285309 |

TABLE XI. $^3P_0$ bottomonium fit parameters, $\mu = m_b$.

| | $a$ | $\xi_0$ | $\sigma^2$ | $\beta$ | $b$ | $c$ |
|---|---|---|---|---|---|---|
| $n = 1$ | 7.88045 | – | – | 1.03344 | 5.01843 | 0.0756304 |
| $n = 2$ | 4.15287 | 0 | 0.0173548 | 1.01512 | −0.173547 | 0.0256279 |
| $n = 3$ | 3.33759 | 0.280277 | 0.0230325 | 1.10439 | 0.283173 | 0.0283235 |

TABLE XII. $^1P_{1\perp}$ charmonium fit parameters, $\mu = \infty$.

| | $a$ | $\xi_0$ | $\sigma^2$ | $\beta$ | $b$ | $c$ |
|---|---|---|---|---|---|---|
| $n = 1$ | 1.78365 | – | – | 1.4891 | 0.636329 | 0.431836 |
| $n = 2$ | 2.43681 | 0.284756 | 0.0966684 | 0.921282 | 0 | – |
| $n = 3$ | 1.53215 | 0.487944 | 0.122605 | 0.734715 | 0.562724 | 0.122482 |

TABLE XIII. $^1P_{1\perp}$ charmonium fit parameters, $\mu = m_c$.

| | $a$ | $\xi_0$ | $\sigma^2$ | $\beta$ | $b$ | $c$ |
|---|---|---|---|---|---|---|
| $n = 1$ | 2.26917 | – | – | 2.14573 | 0.541302 | 0.383543 |
| $n = 2$ | 1.40861 | 0.370795 | 0.0301022 | 0.303023 | 0 | – |
| $n = 3$ | 2.15625 | 0.530031 | 0.0483686 | 0.23274 | 0.269402 | 1.01888 |

TABLE XIV. $^1P_{1\perp}$ bottomonium fit parameters, $\mu = \infty$.

| | $a$ | $\xi_0$ | $\sigma^2$ | $\beta$ | $b$ | $c$ |
|---|---|---|---|---|---|---|
| $n = 1$ | 11.7196 | – | – | 1.74248 | 0.126342 | 0.0638176 |
| $n = 2$ | 1.59483 | 0.12902 | 0.00748694 | 0.1 | 0 | – |
| $n = 3$ | 17.2954 | 0.254288 | 0.0186876 | 2.57763 | 0.18766 | 0.0149827 |

TABLE XV. $^1P_{1\perp}$ bottomonium fit parameters, $\mu = m_b$.

| | $a$ | $\xi_0$ | $\sigma^2$ | $\beta$ | $b$ | $c$ |
|---|---|---|---|---|---|---|
| $n=1$ | 13.3807 | – | – | 1.94856 | 0.120252 | 0.0635912 |
| $n=2$ | 1.61774 | 0.135557 | 0.00687409 | 0.1 | 0 | – |
| $n=3$ | 8.28066 | 0.24319 | 0.0150691 | 1.86152 | 0.242844 | 0.0159363 |

TABLE XVI. $^1P_{1\parallel}$ charmonium fit parameters, $\mu = \infty$.

| | $a$ | $\xi_0$ | $\sigma^2$ | $\beta$ | $b$ | $c$ |
|---|---|---|---|---|---|---|
| $n=1$ | 7.28898 | – | – | 4.6828 | 1.79244 | 0.273028 |
| $n=2$ | 8.65428 | 0.242683 | 0.167489 | 1.86131 | −0.326097 | 0.128336 |
| $n=3$ | 2.8194 | 0.514286 | 0.0924345 | 1.13424 | 0.456194 | 0.0903501 |

TABLE XVII. $^1P_{1\parallel}$ charmonium fit parameters, $\mu = m_c$.

| | $a$ | $\xi_0$ | $\sigma^2$ | $\beta$ | $b$ | $c$ |
|---|---|---|---|---|---|---|
| $n=1$ | 53.6273 | – | – | 2.39208 | 0.155202 | 0.273479 |
| $n=2$ | 10.0745 | 0.269738 | 0.160284 | 1.92211 | −0.426175 | 0.13256 |
| $n=3$ | 2.74678 | 0.516953 | 0.0704437 | 0.980324 | 0.294645 | 0.0616262 |

TABLE XVIII. $^1P_{1\parallel}$ bottomonium fit parameters, $\mu = \infty$.

| | $a$ | $\xi_0$ | $\sigma^2$ | $\beta$ | $b$ | $c$ |
|---|---|---|---|---|---|---|
| $n=1$ | 10.5205 | – | – | 1.50861 | 5.65674 | 0.0638543 |
| $n=2$ | 24.2512 | 0 | 0.0147382 | 2.63148 | −0.199554 | 0.0189217 |
| $n=3$ | 3.28997 | 0.232939 | 0.0123631 | 0.987534 | 0.300752 | 0.0169844 |

TABLE XIX. $^1P_{1\parallel}$ bottomonium fit parameters, $\mu = m_b$.

| | $a$ | $\xi_0$ | $\sigma^2$ | $\beta$ | $b$ | $c$ |
|---|---|---|---|---|---|---|
| $n=1$ | 9.97137 | – | – | 1.52337 | 6.0868 | 0.0639454 |
| $n=2$ | 8.82176 | $1.25\times10^{-6}$ | 0.0113222 | 1.63918 | −0.18903 | 0.0186983 |
| $n=3$ | 18.256 | 0.255062 | 0.0130517 | 2.61225 | 0.240445 | 0.0151002 |

TABLE XX. $^3P_{1\perp}$ charmonium fit parameters, $\mu = \infty$.

| | $a$ | $\xi_0$ | $\sigma^2$ | $\beta$ | $b$ | $c$ |
|---|---|---|---|---|---|---|
| $n=1$ | 47.933 | – | – | 2.33766 | 0.183997 | 0.263943 |
| $n=2$ | 9.78918 | 0.142262 | 0.180577 | 1.92684 | −0.391433 | 0.12737 |
| $n=3$ | 2.62768 | 0.474425 | 0.07959 | 1.05711 | 0.437048 | 0.0611108 |

TABLE XXI. $^3P_{1\perp}$ charmonium fit parameters, $\mu = m_c$.

| | $a$ | $\xi_0$ | $\sigma^2$ | $\beta$ | $b$ | $c$ |
|---|---|---|---|---|---|---|
| $n=1$ | 58.1733 | – | – | 2.42818 | 0.148617 | 0.258012 |
| $n=2$ | 12.3322 | 0.156543 | 0.184174 | 2.02338 | −0.500837 | 0.135897 |
| $n=3$ | 2.71267 | 0.487316 | 0.062559 | 0.966985 | 0.318898 | 0.044592 |

TABLE XXII. $^3P_{1\perp}$ bottomonium fit parameters, $\mu = \infty$.

| | $a$ | $\xi_0$ | $\sigma^2$ | $\beta$ | $b$ | $c$ |
|---|---|---|---|---|---|---|
| $n = 1$ | 460.545 | – | – | 3.96925 | 0.127859 | 0.0535103 |
| $n = 2$ | 24.2512 | 0 | 0.0147382 | 2.63148 | −0.199554 | 0.0189217 |
| $n = 3$ | 1.33436 | 0.207932 | 0.009408 | 0.1 | 0.314583 | 0.0117902 |

TABLE XXIII. $^3P_{1\perp}$ bottomonium fit parameters, $\mu = m_b$.

| | $a$ | $\xi_0$ | $\sigma^2$ | $\beta$ | $b$ | $c$ |
|---|---|---|---|---|---|---|
| $n = 1$ | 460.778 | – | – | 3.98292 | 0.129095 | 0.515475 |
| $n = 2$ | 24.2512 | 0 | 0.0147382 | 2.63148 | −0.199554 | 0.0189217 |
| $n = 3$ | 2.50176 | 0.21579 | 0.00891723 | 0.692022 | 0.312109 | 0.0119042 |

TABLE XXIV. $^3P_{1\parallel}$ charmonium fit parameters, $\mu = \infty$.

| | $a$ | $\xi_0$ | $\sigma^2$ | $\beta$ | $b$ | $c$ |
|---|---|---|---|---|---|---|
| $n = 1$ | 1.89725 | – | – | 0.833424 | 0.531147 | 0.334782 |
| $n = 2$ | 3.59963 | 0.000054 | 0.148262 | 0.571469 | −0.551464 | 0.67177 |
| $n = 3$ | 2.32785 | 0.469035 | 0.109016 | 0.999494 | 0.406331 | 0.0780892 |

TABLE XXV. $^3P_{1\parallel}$ charmonium fit parameters, $\mu = m_c$.

| | $a$ | $\xi_0$ | $\sigma^2$ | $\beta$ | $b$ | $c$ |
|---|---|---|---|---|---|---|
| $n = 1$ | 11.121 | – | – | 1.91255 | 0.0836092 | 0.343286 |
| $n = 2$ | 5.84685 | $1 \times 10^{-8}$ | 0.152987 | 0.33432 | −0.847095 | 0.529515 |
| $n = 3$ | 1.34405 | 0.487261 | 0.0170547 | 0.05 | 0.0564819 | 0.00851709 |

TABLE XXVI. $^3P_{1\parallel}$ bottomonium fit parameters, $\mu = \infty$.

| | $a$ | $\xi_0$ | $\sigma^2$ | $\beta$ | $b$ | $c$ |
|---|---|---|---|---|---|---|
| $n = 1$ | 15.1067 | – | – | 1.99935 | 0.104585 | 0.0630898 |
| $n = 2$ | 1.62749 | 0.129254 | 0.00695058 | 0.1 | 0 | – |
| $n = 3$ | 4.52742 | 0.216833 | 0.0131697 | 1.26096 | 0.233993 | 0.0111891 |

TABLE XXVII. $^3P_{1\parallel}$ bottomonium fit parameters, $\mu = m_b$.

| | $a$ | $\xi_0$ | $\sigma^2$ | $\beta$ | $b$ | $c$ |
|---|---|---|---|---|---|---|
| $n = 1$ | 8.43243 | – | – | 1.68704 | 0.200742 | 0.0638126 |
| $n = 2$ | 1.63952 | 0.133876 | 0.00654186 | 0.1 | 0 | – |
| $n = 3$ | 33.7026 | 0.252602 | 0.0148385 | 3.14863 | 0.181075 | 0.00958596 |

TABLE XXVIII. $^3P_{2\perp}$ charmonium fit parameters, $\mu = \infty$.

| | $a$ | $\xi_0$ | $\sigma^2$ | $\beta$ | $b$ | $c$ |
|---|---|---|---|---|---|---|
| $n = 1$ | 18.9386 | – | – | 1.53348 | 0.588362 | 0.187505 |
| $n = 2$ | 9.78268 | 0.000301 | 0.159954 | 1.92414 | −0.331021 | 0.125204 |
| $n = 3$ | 2.98352 | 0.455036 | 0.0789049 | 1.21573 | 0.49737 | 0.0706649 |

TABLE XXIX. $^3P_{2\perp}$ charmonium fit parameters, $\mu = m_c$.

| | $a$ | $\xi_0$ | $\sigma^2$ | $\beta$ | $b$ | $c$ |
|---|---|---|---|---|---|---|
| $n = 1$ | 23.5577 | – | – | 1.70536 | 0.469824 | 0.191909 |
| $n = 2$ | 6.95313 | 0.2615 | 0.122794 | 1.72871 | −0.251262 | 0.0784634 |
| $n = 3$ | 3.28322 | 0.4731 | 0.0684879 | 1.16459 | 0.309103 | 0.0461067 |

TABLE XXX. $^3P_{2\perp}$ bottomonium fit parameters, $\mu = \infty$.

| | $a$ | $\xi_0$ | $\sigma^2$ | $\beta$ | $b$ | $c$ |
|---|---|---|---|---|---|---|
| $n = 1$ | 5.03627 | – | – | 1.36603 | 12.6441 | 0.066995 |
| $n = 2$ | 54.0733 | 0 | 0.0147382 | 3.38888 | −0.199327 | 0.0189271 |
| $n = 3$ | 4.27052 | 0.223597 | 0.0109257 | 1.21376 | 0.305811 | 0.0155296 |

TABLE XXXI. $^3P_{2\perp}$ bottomonium fit parameters, $\mu = m_b$.

| | $a$ | $\xi_0$ | $\sigma^2$ | $\beta$ | $b$ | $c$ |
|---|---|---|---|---|---|---|
| $n = 1$ | 4.60379 | – | – | 1.34201 | 14.0572 | 0.0666158 |
| $n = 2$ | 22.905 | $1.04 \times 10^{-6}$ | 0.0121405 | 2.55386 | −0.184869 | 0.0175767 |
| $n = 3$ | 7.66472 | 0.231103 | 0.0112419 | 1.75192 | 0.282943 | 0.014799 |

TABLE XXXII. $^3P_{2\parallel}$ charmonium fit parameters, $\mu = \infty$.

| | $a$ | $\xi_0$ | $\sigma^2$ | $\beta$ | $b$ | $c$ |
|---|---|---|---|---|---|---|
| $n = 1$ | 11.3608 | – | – | 1.21471 | 0.697849 | 0.272678 |
| $n = 2$ | 4.44771 | 0.232039 | 0.158319 | 1.41475 | −0.119605 | 0.0808185 |
| $n = 3$ | 2.3202 | 0.461568 | 0.0998141 | 1.01046 | 0.418644 | 0.0858612 |

TABLE XXXIII. $^3P_{2\parallel}$ charmonium fit parameters, $\mu = m_c$.

| | $a$ | $\xi_0$ | $\sigma^2$ | $\beta$ | $b$ | $c$ |
|---|---|---|---|---|---|---|
| $n = 1$ | 14.4417 | – | – | 1.40581 | 0.551405 | 0.278178 |
| $n = 2$ | 8.83337 | 0.173308 | 0.229571 | 1.85411 | −0.360409 | 0.141981 |
| $n = 3$ | 2.51931 | 0.476137 | 0.0902674 | 0.976052 | 0.253069 | 0.0561185 |

TABLE XXXIV. $^3P_{2\parallel}$ bottomonium fit parameters, $\mu = \infty$.

| | $a$ | $\xi_0$ | $\sigma^2$ | $\beta$ | $b$ | $c$ |
|---|---|---|---|---|---|---|
| $n = 1$ | 5.24954 | – | – | 1.11938 | 10.5179 | 0.069816 |
| $n = 2$ | 26.8594 | 0 | 0.0147382 | 2.73992 | −0.168346 | 0.0189217 |
| $n = 3$ | 3.78742 | 0.222412 | 0.0131263 | 1.13605 | 0.259637 | 0.0157952 |

TABLE XXXV. $^3P_{2\parallel}$ bottomonium fit parameters, $\mu = m_b$.

| | $a$ | $\xi_0$ | $\sigma^2$ | $\beta$ | $b$ | $c$ |
|---|---|---|---|---|---|---|
| $n = 1$ | 4.7464 | – | – | 1.09225 | 11.8753 | 0.0695242 |
| $n = 2$ | 26.8594 | 0 | 0.0147382 | 2.73992 | −0.168346 | 0.0189217 |
| $n = 3$ | 2.28 | 0.222311 | 0.0105893 | 0.673188 | 0.326787 | 0.0180464 |

constant in Tables VI and VII. As can be seen from the tables, results obtained in this work for $f_{\mathrm{odd}}$ are larger by about 30% from the results of [24] in both sectors. For $f_{\mathrm{even}}$, the discrepancy is even larger, and results obtained in this work are almost twice as large as the results of [24]. In [23], only the result for $f_{\mathrm{even}}$ for charmonium is available. The result of [23] is in agreement with the result of this work.

In Figs. 1–7, LCDAs are depicted for various states. In each of the plots, LCDAs are obtained using Eqs. (12)–(18) with both $\mu = \infty$ and $\mu = m_q$, and also the fits to the LCDAs for both $\mu$ values are shown. The parameters used for each fit are presented in Tables VIII–XXXV. As can be observed from the figures, the fits reliably reproduce the calculated LCDAs. Some general observations about the DAs are in order. Odd DAs have $2n + 1$ extrema for $u > 0$, reflecting the nodal structure of the wave functions of the excited states. Even DAs have one (three) extrema when $n = 1$ ($n = 2$ or $n = 3$). Some of the extrema for even DAs for $n = 2$ and $n = 3$ are converted into inflection points due to nearby, larger extrema. As $n$ increases, some of the extrema move towards the $\xi = \pm 1$ region. Similarly, the DAs for a given $n$ are localized closer to $\xi = 0$ for bottomonium than for charmonium. This is again a reflection of the highly nonrelativistic nature of the bottomonium system. As expected, another reflection of the nonrelativistic nature of small $n$ and the bottomonium system is the dependence on the scale $\mu$. In general, bottomonium systems and small $n$ systems are more nonrelativistic compared to charmonium and larger $n$ systems.

## IV. CONCLUSIONS

In this work, the three lowest lying states of $p$-wave charmonia and bottomonia have been considered. Their LCDAs and decay constants have been calculated.

It is observed the spin-orbit effects can be important in the determination of the leptonic decay constants. Also, leptonic decay constants and LCDAs exhibit a more significant scale dependence for charmonium than for the bottomonium. The importance of the relativistic contributions becomes also larger as $n$ (the radial excitation quantum number) increases.

Also, the DAs of the bottomonium are closer to the $\xi = 0$ region than the charmonium DAs. Also, as $n$ increases, in both of the sectors DAs shift towards larger values of $|\xi|$.

For future usage, model functions have been fitted to the obtained LCDAs so that the obtained DAs can be easily used in future works.

## ACKNOWLEDGMENTS

This work is partially supported by Türkiye Bilimsel ve Teknolojik Araştırma Kurumu (TUBITAK) under Grant No. 111T706.

[1] D. Gross and F. Wilczek, Phys. Rev. Lett. **30**, 1343 (1973); H. D. Politzer, Phys. Rev. Lett. **30**, 1346 (1973).
[2] P. Colangelo and A. Khodjamirian, in *At the Frontier of Particle Physics* Vol. 3, edited by M. Shifman, p. 1495 (2001), http://www.worldscientific.com/worldscibooks/10.1142/4544.
[3] M. B. Voloshin, Prog. Part. Nucl. Phys. **61**, 455 (2008).
[4] S. Godfrey and N. Isgur, Phys. Rev. D **32**, 189 (1985).
[5] M. A. Shifman, A. I. Vainshtein, and V. I. Zakharov, Nucl. Phys. **B147**, 385 (1979).
[6] I. I. Balitsky, V. M. Braun, and A. V. Kolesnichenko, Nucl. Phys. **B312**, 509 (1989).
[7] P. M. Hohler and R. Rapp, Nucl. Phys. **A892**, 58 (2012).
[8] E. Di Salvo, M. Pallavicini, and E. Robutti, Phys. Lett. B **441**, 447 (1998).
[9] S. Brodsky, Report No. SLAC-PUB-8427, April 2000.
[10] G. P. Lepage, S. J. Brodsky, T. Huang, and P. B. Mackenzie, in *Proceedings of the Banff Summer Institute on Particles and Fields* (Plenum, New York, 1983), p. 83.
[11] G. P. Lepage and S. J. Brodsky, Phys. Rev. D **22**, 2157 (1980).
[12] S. J. Brodsky, arXiv:hep-ph/9807212.
[13] S. J. Brodsky, S. Pinsky, and H. C. Pauli, Phys. Rep. **301**, 299 (1998).
[14] K. Azizi, M. Bayar, A. Ozpineci, and Y. Sarac, Phys. Rev. D **82**, 076004 (2010).
[15] V. M. Belyaev, V. M. Braun, A. Khodjamirian, and R. Ruckl, Phys. Rev. D **51**, 6177 (1995).
[16] V. M. Braun, Report No. NORDITA-98-1-P.
[17] K.-C. Yang, Nucl. Phys. **B776**, 187 (2007).
[18] H.-Y. Cheng, Y. Koike, and K.-C. Yang, Phys. Rev. D **82**, 054019 (2010).
[19] V. V. Braguta, Phys. At. Nucl. **74**, 86 (2011).
[20] V. V. Braguta, Phys. Lett. B **646**, 80 (2007).
[21] V. V. Braguta, Phys. Rev. D **77**, 034026 (2008).
[22] V. V. Braguta, Phys. Rev. D **75**, 094016 (2007).
[23] V. V. Braguta, A. K. Likhoded, and A. V. Luchinsky, Phys. Rev. D **79**, 074004 (2009).
[24] C. W. Hwang, J. High Energy Phys. 10 (2009) 074.
[25] M. Takizawa and S. Takeuchi, Prog. Theor. Exp. Phys. **2013**, 093D01 (2013).
[26] E. Cincioglu, J. Nieves, A. Ozpineci, and A. U. Yilmazer, Eur. Phys. J. C **76**, 576 (2016).
[27] J. Beringer *et al.* (Particle Data Group Collaboration), Phys. Rev. D **86**, 010001 (2012).
[28] T. Huang and F. Zuo, Eur. Phys. J. C **51**, 833 (2007).